

Optimization of Iterative Blind Detection based on Expectation Maximization and Belief Propagation

Luca Schmid*, Tomer Raviv[†], Nir Shlezinger[†], and Laurent Schmalen*

*Communications Engineering Lab, Karlsruhe Institute of Technology, Hertzstr. 16, 76187 Karlsruhe, Germany

[†]School of ECE, Ben-Gurion University of the Negev, Be'er-Sheva, Israel

Email: *first.last@kit.edu, [†]tomerraviv95@gmail.com, nirshl@bgu.ac.il

Abstract—We study iterative blind symbol detection for block-fading linear inter-symbol interference channels. Based on the factor graph framework, we design a joint channel estimation and detection scheme that combines the expectation maximization (EM) algorithm and the ubiquitous belief propagation (BP) algorithm. Interweaving the iterations of both schemes significantly reduces the EM algorithm’s computational burden while retaining its excellent performance. To this end, we apply simple yet effective model-based learning methods to find a suitable parameter update schedule by introducing momentum in both the EM parameter updates as well as in the BP message passing. Numerical simulations verify that the proposed method can learn efficient schedules that generalize well and even outperform coherent BP detection in high signal-to-noise scenarios.

Index Terms—Factor graphs, joint detection, model-based learning, expectation maximization, belief propagation, 6G.

I. INTRODUCTION

We study the application of iterative receivers for joint channel estimation and symbol detection on block-fading linear inter-symbol interference (ISI) channels. Most practical communication systems estimate the current channel state based on a priori known pilot symbols. However, in scenarios with short block length transmission, like low-latency communications in 5G/6G or Internet of Things systems, the pilots occupy a significant part of the short transmission blocks and thus significantly reduce the throughput. This motivates considering *blind* receivers that do not rely on pilot symbols, but estimate the channel state from the statistics of the received signal.

Optimum blind estimation and detection based on the maximum likelihood (ML) criterion [1] is competitive in terms of detection performance with coherent detectors and fully available channel state information (CSI) but suffers from high computational complexity. Alternatively, practical blind detectors with reduced complexity, like the constant modulus algorithm (CMA) [2] or variational methods [3] are still consistently outperformed by coherent detection schemes.

Iterative receivers bear the potential of approximating ML-based joint estimation and detection with an attractive performance-complexity tradeoff [4]. To this end, we study the framework of factor graphs and the belief propagation

(BP) algorithm for joint estimation and detection. One major challenge is the handling of continuous latent variables in the factor graph which typically leads to intractable integrals in the BP update equations. Approaches in the literature combatting this issue vary from quantized BP messages over particle filters [5] to parametrized canonical distributions [4]. For instance, [6] approximates the continuous probability distributions by mixtures of Gaussian distributions. A promising approach was considered in [7], [8], where the expectation maximization (EM) algorithm was used as a message passing algorithm in the factor graph to handle continuous variables.

Inspired by this idea, we integrate the EM algorithm into our BP-based detector for joint estimation and detection. In contrast to [8], we do not apply EM as a local message update rule but instead perform global EM parameter updates which turn out to be more efficient in terms of complexity. The combination of two iterative schemes like the EM and BP algorithm raises the question of suitable update schedules which have a significant impact on both performance and complexity. To this end, we unfold the iterations of the EM and BP algorithm as a form of model-based deep learning [9], [10] and introduce momentum in the updates by a convex combination with former values. Thereby, the schedule is fully defined by a set of continuous momentum weights which can be learned in an end-to-end manner via gradient-based optimization. Our numerical experiments show that the optimized schedule can substantially reduce the number of necessary EM steps by allowing parallel parameter updates while preserving the stability of the EM algorithm. In a similar manner, momentum can improve the convergence behavior of BP which leads to an improved detection performance.

II. SYSTEM MODEL AND PRELIMINARIES

A. Channel Model

We study the transmission over a block-fading channel in the digital baseband which is impaired by linear ISI and additive white Gaussian noise (AWGN) [11]. The channel state is constant for a block of N consecutively transmitted information symbols $\mathbf{c} \in \mathcal{M}^N$, where each symbol c_n is sampled independently and uniformly from a multilevel constellation $\mathcal{M} = \{\mathbf{c}_i \in \mathbb{C}, i = 1, \dots, M\}$. The receiver observes the sequence

$$\mathbf{y} = \mathbf{H}\mathbf{c} + \mathbf{w}, \quad \mathbf{H} \in \mathbb{C}^{N+L \times N}$$

This work has received funding in part from the European Research Council (ERC) under the European Union’s Horizon 2020 research and innovation programme (grant agreement No. 101001899), in part from the German Federal Ministry of Education and Research (BMBF) within the project Open6GHub (grant agreement 16KISK010), and in part from the Israeli Ministry of Science and Technology.

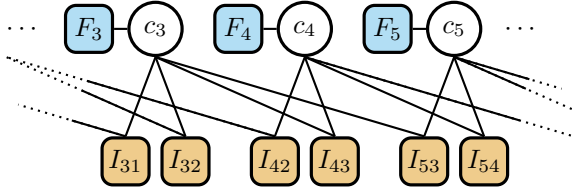


Fig. 1: Factor graph representation of (2) for a channel with memory $L = 2$.

where \mathbf{H} is the band-structured Toeplitz matrix that represents the convolution of \mathbf{c} with the impulse response of the linear ISI channel $\mathbf{h} = (h_0, \dots, h_L)^T \in \mathbb{C}^{L+1}$. The vector \mathbf{w} contains independent noise samples $w_n \sim \mathcal{CN}(0, \sigma^2)$ from a complex circular Gaussian distribution. For each transmission block, the channel is thus fully characterized by the parameter vector $\boldsymbol{\theta} := (h_0, \dots, h_L, \sigma^2)^T$ of length $L + 2$, which is independently sampled in each block. We define the signal-to-noise ratio (SNR) at the receiver as

$$\text{snr} := \frac{\|\mathbf{h}\|^2 \cdot \mathbb{E}_{\mathbf{c}}\{\|\mathbf{c}\|^2\}}{\mathbb{E}_{\mathbf{w}}\{\|\mathbf{w}\|^2\}}.$$

We study *blind* channel estimation and joint symbol detection, i.e., the parameters $\boldsymbol{\theta}$ are unknown to both the transmitter and the receiver. The goal is to infer the channel state $\boldsymbol{\theta}$ and the transmitted symbols \mathbf{c} from the observation \mathbf{y} .

B. Factor Graph-based Symbol Detection

As a basis for iterative reception, we consider the powerful framework of factor graphs and the BP algorithm [4], [12]. We focus on a detection algorithm with particularly low computational complexity [13], which we introduce in the following. For a more detailed elaboration of this detector, we refer the reader to [13], [14].

Maximum a posteriori (MAP) detection is based on the a posteriori probability (APP) distribution $P(\mathbf{c}|\mathbf{y})$. Assuming uniformly distributed transmit symbols, the latter can be written as

$$P(\mathbf{c}|\mathbf{y}) \propto p(\mathbf{y}|\mathbf{c}) \propto \exp\left(\frac{2\text{Re}\{\mathbf{c}^H \mathbf{x}\} - \mathbf{c}^H \mathbf{G} \mathbf{c}}{\sigma^2}\right), \quad (1)$$

by defining $\mathbf{x} := \mathbf{H}^H \mathbf{y}$ and $\mathbf{G} := \mathbf{H}^H \mathbf{H}$ as the matched filtered versions of the observation and the channel matrix, respectively. The proportionality \propto in (1) indicates that the terms are only differing in a factor independent of \mathbf{c} . Equation (1) can be written in factorized form

$$P(\mathbf{c}|\mathbf{y}) \propto \prod_{n=1}^N \left[F_n(c_n) \prod_{m=1}^{n-1} I_{nm}(c_n, c_m) \right], \quad (2)$$

where we introduced the local factors

$$F_n(c_n) := \exp\left\{\frac{1}{\sigma^2} \text{Re}\{2x_n c_n^* - G_{nn} |c_n|^2\}\right\} \quad (3)$$

$$I_{nm}(c_n, c_m) := \exp\left\{-\frac{2}{\sigma^2} \text{Re}\{G_{nm} c_m c_n^*\}\right\}. \quad (4)$$

The factor graph representation of (2) is shown in Fig. 1. Applying the BP algorithm with a parallel schedule on the factor graph in Fig. 1 yields an iterative algorithm for symbol detection. We denote by $\mu_{nm}^{(t)}(c_m)$ a BP message from variable c_n to c_m in iteration t . After a uniform initialization of all messages $\mu_{nm}^{(0)}(c_m) = 1$, the iterative BP updates read for $t = 1, \dots, T$ as

$$b_n^{(t)}(c_n) = \gamma_n^{(t)} \prod_{k \neq n} \mu_{kn}^{(t)}(c_n), \quad (5)$$

$$\mu_{nm}^{(t+1)}(c_m) = \sum_{c_n} I_{nm}(c_n, c_m) F_n(c_n) \frac{b_n^{(t)}(c_n)}{\mu_{mn}^{(t)}(c_n)}, \quad (6)$$

where $\gamma_n^{(t)} \in \mathbb{R}$ is a normalization constant such that $b_n^{(t)}(c_n)$ is a normalized probability distribution.¹ Because the factor graph in Fig. 1 contains cycles, the beliefs $b_n(c_n)$ are only an approximation of the APP distributions $P(c_n|\mathbf{y})$ and the quality of approximation strongly depends on the underlying channel characteristics [14].

III. BLIND ESTIMATION AND DETECTION VIA EM AND BP

The detection algorithm in Sec. II-B relies on the availability of CSI in the definition of the factors (3) and (4). To enable blind detection, we propose an iterative joint estimation and detection scheme by integrating the EM algorithm into the iterative receiver. EM is an established method for finding ML parameter estimates in probabilistic models that contain latent variables [15]. The log-likelihood function can be written as

$$\begin{aligned} \log p(\mathbf{y}|\boldsymbol{\theta}) &= \log p(\mathbf{c}, \mathbf{y}|\boldsymbol{\theta}) - \log P(\mathbf{c}|\mathbf{y}, \boldsymbol{\theta}) \\ &= \underbrace{\sum_{\mathbf{c}} Q(\mathbf{c}) \log\left(\frac{p(\mathbf{c}, \mathbf{y}|\boldsymbol{\theta})}{Q(\mathbf{c})}\right)}_{=: \mathcal{L}(Q, \boldsymbol{\theta})} - \underbrace{\sum_{\mathbf{c}} Q(\mathbf{c}) \log\left(\frac{P(\mathbf{c}|\mathbf{y}, \boldsymbol{\theta})}{Q(\mathbf{c})}\right)}_{=: D_{\text{KL}}(Q\|P) \geq 0}, \end{aligned}$$

where $Q(\mathbf{c})$ is a normalized trial distribution of \mathbf{c} . The EM algorithm maximizes the evidence lower bound (ELBO) $\mathcal{L}(Q, \boldsymbol{\theta}) \leq \log p(\mathbf{y}|\boldsymbol{\theta})$ in a 2-stage iterative algorithm. Starting with an initial guess for the parameters $\hat{\boldsymbol{\theta}}^{(0)}$, the EM algorithm iteratively performs for $t = 1, \dots, T$

1) **E-step:** Evaluate

$$Q^{(t)}(\mathbf{c}) = P(\mathbf{c}|\mathbf{y}, \hat{\boldsymbol{\theta}}^{(t-1)}), \quad (7)$$

2) **M-step:** Compute

$$\hat{\boldsymbol{\theta}}^{(t)} = \arg \max_{\boldsymbol{\theta}} \mathcal{L}(Q^{(t)}, \boldsymbol{\theta}). \quad (8)$$

The EM algorithm monotonically increases the log-likelihood $\log p(\mathbf{y}|\hat{\boldsymbol{\theta}}^{(t)})$ in every iteration t , however, it is not guaranteed to converge to the global maximum [7].

We apply the EM algorithm to the considered problem in Sec. II-A. The E-step in (8) requires the computation of the APP distribution $Q^{(t)}(\mathbf{c}) = P(\mathbf{c}|\mathbf{y}, \hat{\boldsymbol{\theta}}^{(t-1)})$, which relates to the MAP symbol detection task discussed in Sec. II-B. To

¹Note that in practical implementations, the BP algorithm is typically carried out in the logarithmic domain for improved numerical stability and reduced computational complexity.

$$\begin{aligned}\hat{\sigma}^{2(t)} &= \frac{1}{N} \left[\sum_{n=1}^{N+L} |y_n|^2 - \sum_{n=1}^N \sum_{c_n} b_n^{(t)}(c_n) \left(2\text{Re} \{x_n c_n^*\} - G_{nn} |c_n|^2 - \sum_{m < n} \sum_{c_m} b_m^{(t)}(c_m) 2\text{Re} \{G_{mn} c_m c_n^*\} \right) \right], \\ \hat{h}_\ell^{(t)} &= \left(\sum_{n=1}^N \sum_{c_n} b_n^{(t)}(c_n) (y_{n+\ell} c_n^*) - \sum_{\substack{k=0 \\ k \neq \ell}}^L \sum_{c_{n-|\ell-k|}} b_{n-|\ell-k|}^{(t)}(c_{n-|\ell-k|}) h_k^{(t-1)} \right. \\ &\quad \left. \left(\text{Re} \{c_{n-|\ell-k|} c_n^*\} - j \cdot \text{Im} \{c_{n-|\ell-k|} c_n^*\} \text{sign} \{\ell - k\} \right) \right) \cdot \left(\sum_{n=1}^N \sum_{c_n} b_n^{(t)}(c_n) |c_n|^2 \right)^{-1}\end{aligned}\quad (9)$$

reduce the computational complexity, we consequently use the BP-based symbol detector to efficiently perform the E-step by approximating the symbol-wise posteriors $P(c_n | \mathbf{y}, \hat{\boldsymbol{\theta}}^{(t-1)})$ with the beliefs $b_n(c_n)$. Thereby, the complexity only scales linearly with L , instead of exponentially. For the optimization (8) in the M-step, we follow a coordinate descent maximization. By solving $(\partial/\partial\theta_i)\mathcal{L}(b_n(c_n)^{(t)}, \boldsymbol{\theta}) = 0$ for every θ_i , we can find the optimal update rules for each dimension θ_i in closed form, respectively. The resulting EM parameter updates are given in (9)-(10), and scale with $\mathcal{O}(NLM^2)$ and $\mathcal{O}(NL^2M)$, respectively. A detailed derivation is provided in the full version of this paper [16].

A. Optimizing the EM Parameter Update Schedule

The EM parameter updates directly depend on each other, e.g., the update of $\hat{h}_\ell^{(t)}$ in (10) is a function of $\hat{h}_k^{(t-1)}$ with $k \neq \ell$. This raises the question of a suitable schedule, i.e., which parameters of $\boldsymbol{\theta}$ to update simultaneously in which iteration t of the EM algorithm. Learning a schedule is a discrete and combinatorial problem that is in general non-trivial. We simplify the problem by first converting the schedule learning task into a continuous optimization problem which is then combined with a simple pruning strategy. Therefore, we replace the original EM parameter estimates $\hat{\theta}_k^{(t)}$ by a convex combination of old and new estimates $\beta_{\text{EM},k}^{(t)} \hat{\theta}_k^{(t)} + (1 - \beta_{\text{EM},k}^{(t)}) \hat{\theta}_k^{(t-1)}$ where we have introduced the continuous weights $(\beta_{\text{EM},1}^{(t)}, \dots, \beta_{\text{EM},L+2}^{(t)})^T =: \boldsymbol{\beta}_{\text{EM}}^{(t)} \in \mathbb{R}^{L+2}$, $t = 1, \dots, T$. Note that $\beta_{\text{EM},k}^{(t)} = 1$ corresponds to a full update of the parameter estimate $\hat{\theta}_k$, and $\beta_{\text{EM},k}^{(t)} = 0$ means that this parameter is not updated at all in the EM step t .

We optimize the weights $\boldsymbol{\beta}_{\text{EM}}^{(t)}$ based on a training data set

$$\mathcal{D} = \{(\mathbf{c}^{(d)}, \boldsymbol{\theta}^{(d)}, \mathbf{y}^{(d)}) : d = 1, \dots, D\},$$

which consists of randomly and independently sampled information sequences $\mathbf{c}^{(d)}$, channel realizations $\boldsymbol{\theta}^{(d)}$, and the corresponding noisy channel observations $\mathbf{y}^{(d)}$. By unrolling the EM iterations t into a trainable discriminative machine learning architecture [17], we tune the weights $\boldsymbol{\beta}_{\text{EM}}^{(t)}$ based on \mathcal{D} using backpropagation and the Adam algorithm [18].

Objective functions for end-to-end optimization can either focus on the estimation or the detection performance. For the latter, we use the bitwise mutual information (BMI) as

a maximum achievable information rate between the channel input and the output of the symbol detector [19]. As a loss function for the channel estimation task, we consider the squared estimation error

$$\|\hat{\mathbf{h}} - \mathbf{h}\|^2 = \sum_{\ell=0}^L |\hat{h}_\ell - h_\ell|^2$$

of the channel impulse response \mathbf{h} .

To limit the overall number of parameter updates $K_{\text{EM}} < T \cdot (L + 2)$, we add the L_1 loss

$$\mathcal{L}_{\text{EM}}(K') := \sum_{\beta_k \in \beta_{\text{min}}(K')} |\beta_k|$$

that is known to encourage the sparsity of the coefficients to the original loss function. We denote by $\beta_{\text{min}}(K')$ the set of K' scalar elements in the vectors $\boldsymbol{\beta}_{\text{EM}}^{(t)}$, $t = 1, \dots, T$ with the smallest absolute value. Thereby, the regularization penalizes more than $T \cdot (L + 2) - K'$ parameter updates by enforcing K' scalar elements of the vectors $\boldsymbol{\beta}_{\text{EM}}^{(t)}$, $\forall t$ to be close to zero, i.e., they are effectively not updated. During training, we initialize $K' = 0$ and gradually increase K' until the target number of parameter updates $K_{\text{EM}} = T \cdot (L + 2) - K'$ is reached. After the training procedure, we implement the learned schedule by setting the K' elements in $\beta_{\text{min}}(K')$ to zero. This effectively reduces the complexity since K' less parameter update computations via (9) or (10) need to be carried out. For the remaining parameter updates, we apply the learned momentum weights $\boldsymbol{\beta}_{\text{EM}}^{(t)}$ as a simple and low-complexity generalization of the full EM updates ($\beta_{\text{EM}}^{(t)} = 1$).

B. Enhancing BP Accuracy

The concept of momentum can also be applied to the BP algorithm. By only partially updating the BP messages in each iteration, the convergence behavior can be significantly improved, while retaining the same BP fixed points [20]. As opposed to Sec. III-A, we apply only one momentum weight $\beta_{\text{BP}}^{(t)} \in \mathbb{R}$ per BP message passing iteration $t = 1, \dots, T$. Compared to other neural enhancement techniques like *neural BP* that assign an individual weight to every edge in the unrolled factor graph [21], [14], we expect our model to better generalize to a broad range of channel characteristics instead of specializing in one specific channel.

Algorithm 1: EMBP

Data: $\mathbf{y}, \hat{\boldsymbol{\theta}}^{(0)}$

- 1 $\mu_{nm}^{(0)}(x_m) = 1, b_n^{(0)}(x_n), \quad n, m = 1, \dots, N, n \neq m$
- 2 **for** $t = 1, \dots, T$ **do**
- 3 **E-step:** BP message passing
- 4 Compute messages $\mu_{nm}^{(t)}(c_m)$ using (6)
- 5 $\mu_{nm}^{(t)}(c_m) \leftarrow \beta_{\text{BP}}^{(t)} \mu_{nm}^{(t)}(c_m) + (1 - \beta_{\text{BP}}^{(t)}) \mu_{nm}^{(t-1)}(c_m)$
- 6 Compute beliefs $b_n^{(t)}(c_n)$ based on (5)
- 7 **M-step:** Update parameter estimates
- 8 Compute $\hat{\boldsymbol{\theta}}^{(t)}$ using (9) and (10)
- 9 $\hat{\boldsymbol{\theta}}^{(t)} \leftarrow \beta_{\text{EM}}^{(t)} \odot \hat{\boldsymbol{\theta}}^{(t)} + (1 - \beta_{\text{EM}}^{(t)}) \odot \hat{\boldsymbol{\theta}}^{(t-1)}$

Result: $\hat{\boldsymbol{\theta}} = \hat{\boldsymbol{\theta}}^{(T)}, b_n(c_n) = b_n^{(T)}(c_n)$

C. The EMBP Algorithm

We summarize the proposed blind estimation and joint detection scheme in Alg. 1. Since it combines message passing iterations from the BP algorithm with EM parameter update steps, we denote it the *EMBP algorithm*. For the required initialization of the parameters $\hat{\boldsymbol{\theta}}^{(0)}$, we found that the variational autoencoder-based linear equalizer (VAE-LE), a lightweight blind channel equalizer [3], can provide a robust and convenient initialization.

IV. SIMULATION STUDY

The numerical simulations in this section consider the transmission blocks to contain $N = 100$ symbols from a binary phase-shift keying (BPSK) constellation. For initialization of the EMBP algorithm, we apply 10 iterations of the VAE-LE algorithm [3] with a linear equalization filter of length $2L + 1$.

We evaluate the detection performance of the EMBP algorithm in terms of the bit error rate (BER) over the SNR in Fig. 2 for 10^7 random channels with memory $L = 2$. Note that despite the relatively short channel impulse response length $L + 1 = 3$, the sampled channels can introduce strong ISI where linear detectors like the finite impulse response (FIR) filter of the VAE-LE have limited performance [11]. This can also be observed in Fig. 2, where the VAE-LE is significantly outperformed by the EMBP detector. For the latter, we do not yet apply the momentum-based optimization techniques introduced in Sec. III-A and III-B. Instead, we use a serial parameter update schedule, i.e., every EM step only updates one parameter. We use $T = 3 \cdot (L + 2)$ iteration which means that every parameter θ_k is updated 3 times. We also disable the momentum in the BP message passing by fixing $\beta_{\text{BP}}^{(t)} = 1$ for all t . A surprising observation in Fig. 2 is that the blind EMBP algorithm clearly outperforms the coherent BP detector for $\text{snr} > 3$ dB. At first glance, it might seem counterintuitive that a blind detector can outperform its coherent counterpart which has full access to the CSI. However, the suboptimality of the BP algorithm on cyclic factor graphs directly and heavily depends on the characteristics of the underlying channel assumption. In the full version of this paper [16], we could demonstrate that it is an inherent property

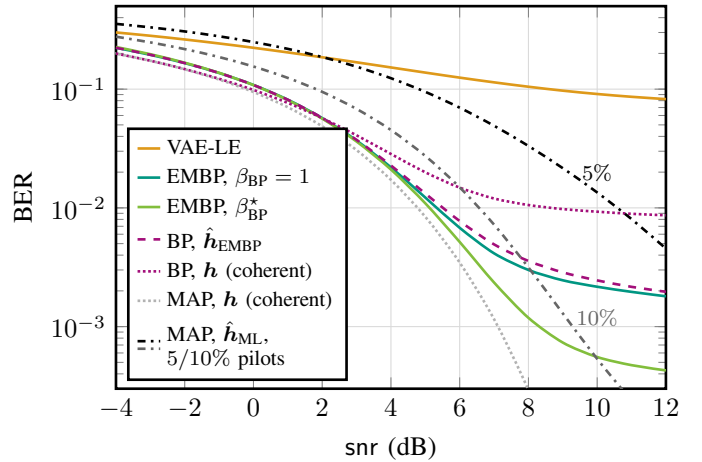


Fig. 2: BER over snr for various detection schemes, averaged over 10^7 random channels with $L = 2$. For the EMBP algorithm, a fixed serial EM update schedule is applied.

of the EM algorithm to converge to a “surrogate” channel representation that deviates from the true channel such that it is better suited for BP-based detection [16]. This is also confirmed in Fig. 2, where the original BP detector based on the channel estimate $\hat{\mathbf{h}}_{\text{EMBP}}$ of the EMBP algorithm performs similarly to the EMBP algorithm itself.

We compare the results of the blind EMBP detector to MAP detection based on a pilot-aided channel estimation. To this end, we fix a portion of the N information symbols in the transmission block to pseudo-random pilot symbols that are known at the receiver. Based on these pilot symbols, the receiver performs ML estimation of \mathbf{h} . Figure 2 shows that the EMBP algorithm clearly outperforms the MAP detector where 5% of the transmission symbols are pilot symbols. For a target BER of 10^{-2} , the EMBP detector also outperforms the baseline with 10% pilots with a 1 dB gain. In the high SNR regime, we observe that the dominant source of error for the EMBP algorithm is the suboptimality of the BP detector. Many short cycles in the underlying factor graph can cause a non-convergent behavior of the BP algorithm, especially for high SNR [14]. To reduce this error floor, we can leverage the momentum-based BP message updates as introduced in Sec. III-B. We optimize the weights $\beta_{\text{BP}}^{(t)}, t = 1, \dots, L + 2 = 12$ for generic channels, i.e., each sample in the training data set \mathcal{D} consists of an independent channel realization and the snr is uniformly sampled in $[0 \text{ dB}, 12 \text{ dB}]$. This generic training can be performed offline and prior to evaluation. We apply batch gradient descent optimization with 200 batches each containing 1000 transmission blocks. As shown in Fig. 2, the EMBP algorithm with optimized momentum weights β_{BP}^* can effectively reduce the error floor by almost one order of magnitude.

We further study the capability of the proposed method to learn an effective EM update schedule that reduces the computational complexity of the EMBP algorithm. We consider a transmission over randomly sampled channels with memory $L = 5$ and optimize the EMBP algorithm towards

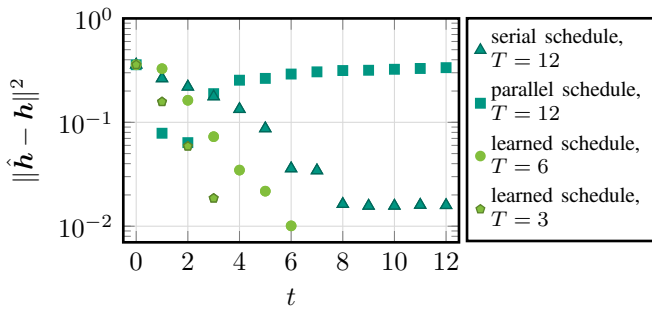


Fig. 3: Mean squared estimation error $\|\hat{\mathbf{h}} - \mathbf{h}\|^2$ after each iteration of the EMBP algorithm with different EM parameter update schedules. The randomly sampled channels have $\text{snr} = 10$ dB and memory $L = 5$, i.e., 7 parameters to estimate (including σ^2).

minimum mean squared error (MSE) of the EMBP channel estimates $\hat{\mathbf{h}}$ while restraining the algorithm’s complexity. More specifically, we limit the EM iterations to $T = 6$ or $T = 3$, respectively. Based on this restriction $T < L + 2 = 7$, the EMBP algorithm would not be able to update each parameter (including σ^2) at least once if it followed a serial update schedule where only one parameter is updated per EM step. We apply the gradient-based end-to-end training method detailed in Sec. III-A to find a more effective EM update schedule for this setting. We use 2500 batches for offline training and each batch contains 1000 random channel realizations. For the schedule learning, we fix the maximum number of parameter updates to $K_{\text{EM}} = 24$.

Figure 3 evaluates the squared channel estimation error over the EMBP iterations t for different EM update schedules. The results are averaged over 10^5 random channels with $\text{snr} = 10$ dB. For the serial schedule, the MSE monotonically decreases with the EMBP iterations t . The stagnation at $t = 7$ is due to the parameter estimate $\hat{\sigma}^2$ not being *directly* included in the evaluation of the squared error $\|\hat{\mathbf{h}} - \mathbf{h}\|^2$. The second baseline in Fig. 3 uses a parallel schedule for EMBP, i.e., all parameters are simultaneously updated in every EM step t . As a result, the MSE decreases significantly after the first EM iteration but worsens after $t = 2$ due to an unstable behavior of the fully parallel updates. The EMBP algorithm with optimized update schedules shows a fast yet stable convergence and the estimation results are comparable to those of the serial EM schedule but with less iterations, i.e., with a reduced computational complexity. The analysis of the learned schedules revealed that only a few parameters are partially updated with small weights β_{EM} in the early EM iterations while the last iterations contain full and parallel updates.

V. CONCLUSION

We proposed the EMBP algorithm for blind channel estimation and joint symbol detection. Combining two iterative inference schemes, EM for estimation and BP for detection, yields a joint estimation and detection scheme with superior performance and low complexity. It further poses the challenge of optimizing the interaction between the iterations of both

algorithms. For the EMBP algorithm, we found the concept of momentum as a particularly simple and effective method to improve an iterative model while retaining an algorithm that generalizes well.

REFERENCES

- [1] M. Ghosh and C. L. Weber, “Maximum-likelihood blind equalization,” *Optical Engineering*, vol. 31, no. 6, pp. 1224–1228, 1992.
- [2] D. Godard, “Self-recovering equalization and carrier tracking in two-dimensional data communication systems,” *IEEE Trans. Commun.*, vol. 28, no. 11, pp. 1867–1875, 1980.
- [3] V. Lasinger, F. Buchali, and L. Schmalen, “Blind equalization and channel estimation in coherent optical communications using variational autoencoders,” *IEEE J. Sel. Areas Commun.*, vol. 40, no. 9, pp. 2529–2539, Sep. 2022.
- [4] A. Worthen and W. Stark, “Unified design of iterative receivers using factor graphs,” *IEEE Transactions on Information Theory*, vol. 47, no. 2, pp. 843–849, Feb. 2001.
- [5] H.-A. Loeliger, “Some remarks on factor graphs,” in *Proc. Int. Symposium Turbo Codes and Related Topics (ISTC)*, Brest, France, Sep. 2003, pp. 111–115.
- [6] Y. Liu, L. Brunel, and J. J. Boutros, “Joint channel estimation and decoding using Gaussian approximation in a factor graph over multipath channel,” in *Proc. IEEE Int. Symp. Pers. Indoor Mobile Radio Commun. (PIMRC)*, Tokyo, Japan, Sep. 2009, pp. 3164–3168.
- [7] A. W. Eckford, “Channel Estimation in Block Fading Channels Using the Factor Graph EM Algorithm,” in *Proc. Biennial Symposium on Communications*, Kingston, Ontario, Canada, May 2004.
- [8] J. Dauwels, S. Korf, and H.-A. Loeliger, “Expectation maximization as message passing,” in *Proc. IEEE Int. Symp. Inf. Theory (ISIT)*, Adelaide, Australia, Sep. 2005, pp. 583–586.
- [9] N. Shlezinger, J. Whang, Y. C. Eldar, and A. G. Dimakis, “Model-based deep learning,” *Proc. IEEE*, vol. 111, no. 5, pp. 465–499, May 2023.
- [10] N. Shlezinger, Y. C. Eldar, and S. P. Boyd, “Model-based deep learning: On the intersection of deep learning and optimization,” *IEEE Access*, vol. 10, pp. 115 384–115 398, 2022.
- [11] J. Proakis and M. Salehi, *Digital Communications*, 5th ed. McGraw Hill, Nov. 2007.
- [12] F. R. Kschischang and H.-A. Loeliger, “Factor graphs and the sum-product algorithm,” *IEEE Trans. Inf. Theory*, vol. 47, no. 2, pp. 498–519, Feb. 2001.
- [13] G. Colavolpe, D. Fertonani, and A. Piemontese, “SISO detection over linear channels with linear complexity in the number of interferers,” *IEEE J. Sel. Topics Signal Process.*, vol. 5, no. 8, pp. 1475–1485, 2011.
- [14] L. Schmid and L. Schmalen, “Low-complexity near-optimum symbol detection based on neural enhancement of factor graphs,” *IEEE Trans. Commun.*, pp. 7562–7575, Nov. 2022.
- [15] A. P. Dempster, N. M. Laird, and D. B. Rubin, “Maximum likelihood from incomplete data via the EM algorithm,” *J. Roy. Stat. Soc.: Ser. B*, vol. 39, no. 1, pp. 1–38, Sep. 1977.
- [16] L. Schmid, T. Raviv, N. Shlezinger, and L. Schmalen, “Blind channel estimation and joint symbol detection with data-driven factor graphs,” *arXiv preprint arXiv:2401.12627*, Jan. 2024.
- [17] N. Shlezinger and T. Rottenberg, “Discriminative and generative learning for linear estimation of random signals [lecture notes],” *IEEE Signal Process. Mag.*, vol. 40, no. 6, pp. 75–82, 2023.
- [18] D. P. Kingma and J. Ba, “Adam: A method for stochastic optimization,” in *Proc. Int. Conf. Learn. Represent. (ICLR)*, San Diego, CA, USA, May 2015.
- [19] A. Alvarado, T. Fehenberger, B. Chen, and F. M. J. Willems, “Achievable information rates for fiber optics: Applications and computations,” *J. Lightw. Technol.*, vol. 36, no. 2, pp. 424–439, Jan. 2018.
- [20] K. Murphy, Y. Weiss, and M. I. Jordan, “Loopy belief propagation for approximate inference: An empirical study,” in *Proc. Int. Conf. Uncertainty Artif. Intell. (UAI)*, Stockholm, Sweden, 1999, pp. 467–475.
- [21] E. Nachmani, E. Marciano, L. Lugosch, W. J. Gross, D. Burshtein, and Y. Beery, “Deep learning methods for improved decoding of linear codes,” *IEEE J. Sel. Topics Signal Process.*, vol. 12, no. 1, pp. 119–131, Feb. 2018.